

# SUPPORT LOSS IN MICROMECHANICAL DISK RESONATORS

Zhili Hao and Farrokh Ayazi

Integrated MEMS Laboratory, School of Electrical and Computer Engineering,  
Georgia Institute of Technology, 777 Atlantic Drive, Atlanta, GA 30332-0250, USA

## ABSTRACT

In light of recent efforts to implement micromechanical resonators with high- $Q$  and high frequency, an analytical model for support loss in micromechanical disk resonators has been developed and verified with experimental results. The derived model is general and applicable to various structures and support schemes (side-supported and center-supported disks), providing significant insight to the geometrical design and choice of materials in high- $Q$  disk resonant structures. The methodology presented in this paper can be extended to evaluate support loss in other high-frequency bulk-mode structures such as length-extensional blocks and bars.

## 1. INTRODUCTION

The mechanical quality factor ( $Q$ ) of a resonator is defined as:

$$Q = 2\pi \cdot \frac{W}{\Delta W} \quad (1)$$

where  $\Delta W$  denotes the energy dissipated per cycle of vibration and  $W$  denotes the maximum vibration energy stored per cycle [1].

A higher  $Q$  in a resonator translates to higher frequency selectivity, improved stability, and lower equivalent impedance (motional resistance). Many dissipation mechanisms exist in micromechanical resonators, such as air damping, thermoelastic damping (TED), surface loss, and support loss. The measured unloaded  $Q$  is mainly the combination of these dissipation mechanisms, expressed as:

$$\frac{1}{Q} = \frac{1}{Q_{air}} + \frac{1}{Q_{TED}} + \frac{1}{Q_{support}} + \frac{1}{Q_{surface}} \quad (2)$$

With the increasing demand for micromechanical resonators with very high frequencies and very high  $Q$ , bulk-mode capacitive disk resonators [2, 3] become an interesting alternative to beam resonators due to their ultra-high stiffness. Among the loss mechanisms in a disk resonator, air damping can be eliminated by operating the resonator in vacuum, while surface loss is negligible due to normally large surface-to-volume ratios. TED does not limit the  $Q$  of the disk resonator throughout the entire VHF and UHF range ( $Q_{TED} \gg Q_{support}$ ) [4]. So far, support loss has been identified as the dominant loss mechanism in the disk resonator [2, 3]. The analytical solution to support loss in this type

of resonators has not yet been studied, although experimental work has begun to address the issue [2, 3].

Support loss, also known as anchor loss, is the portion of the vibration energy of a resonator dissipated by transmission through its support. During its resonant vibrations, a resonant structure exerts a time-harmonic load on its support structure. Acting as an excitation source, this time-harmonic load will further excite elastic waves propagating into the support. Part of the vibration energy dissipated through elastic wave propagation in support media is commonly referred to as *support loss*.

In this work, by extending the analytical methodology that we had previously developed for support loss in beam resonators [1], closed-form expressions for support loss in disk resonators have been derived and verified with numerous test data, providing significant insight to the geometrical design and choice of materials in high- $Q$  disk resonators.

## 2. THEORETICAL ANALYSIS

The bulk-mode vibrations of a free-edged disk have their resonant nodes located at the periphery and/or center of the disk. By locating a support beam at one of such resonant nodes, the disk can be mechanically supported while having small interaction with its support media. Depending on the fabrication technology used, two types of support schemes have been implemented for a disk resonator: 1) side-supported at a resonant node along its periphery, 2) center-supported at its center node. Side-supported disks are easier to implement and compatible with both surface and bulk micromachining technologies. While 3-20 $\mu\text{m}$  thick side-supported single crystal silicon (SCS) disk resonators have been demonstrated through the HARPSS-on-SOI process [2], a number of center-supported poly-diamond disk resonators have been developed with surface micromachining technology [3].

### *Analytical methodology*

In this work, it is assumed that the disk of radius  $R$  is homogeneous, isotropic, and under 2D plane-stress; thus its vibration variables are independent of its thickness. With the origin set at the center of the disk, the plane polar coordinates  $r$  and  $\theta$  is used. Generally, the support beam is much smaller in size than the disk and has negligible effect on the resonant frequency and mode shape of the disk. Hence, the disk can be modeled

as a free-edged circular thin-plate, leading to explicit expressions for its mode shapes and vibration energy.

The deformation at the disk end of the support beam follows the vibrations of the disk and can be calculated from the mode shapes of the disk. As illustrated in Fig. 1, through the support beam, this deformation is further transferred into the stress on the support structure (substrate). It is this resonating stress that acts as an excitation source for the elastic waves in the support structure and induces support loss.

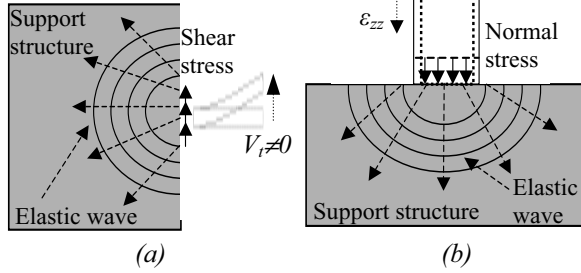


Figure 1. The process of support loss in (a) a side-supported and (b) a center-supported disk resonator

In order to quantitatively evaluate the support loss in a disk resonator in terms of its geometry and resonant mode, the support structure is modeled as a semi-infinite medium, through which part of the vibration energy propagates to infinity and can not return to the resonator, leading to energy loss. The behavior of the support structure can be described by the elastic wave theory, giving rise to the displacement under the resonating stress. Support loss is further formulated as the integral of the product of the stress and its corresponding displacement in the support over one cycle across the clamped region.

The analytical methodology for evaluating support loss in a disk resonator is summarized as follows:

- 1) The bulk-mode vibrations of the free-edged disk are described using the circular thin-plate theory to obtain their resonant frequencies, mode shapes, and vibration energy.
- 2) The support beam is modeled as either a cantilever or a longitudinal rod in order to transfer the deformation at its disk end into the stress on the substrate at its clamped end.
- 3) The support structure is modeled as a semi-infinite medium to calculate the displacement under the stress.
- 4) The stress and the displacement yield the formula for support loss  $\Delta W$  and further lead to the closed-form expression for support quality factor  $Q_{support}$  from the definition of  $Q$ .

### Side-supported disk resonators

Fig. 2(a) shows a side-supported disk resonator of radius  $R$ , clamped to the substrate through a side support beam of width  $b$ , length  $L$ , [5, 6]. Both the disk and the beam have the same thickness  $t$ . With the beam located at one of its resonant nodes along its periphery, this disk resonator operates in its elliptic bulk-mode, as shown in Fig. 2(c). The elliptic mode vibrations consist of the radial ( $U$ ) and circumferential ( $V$ ) displacements, expressed as below [5]:

$$U = \frac{A \cdot \cos(2\theta)}{R} \cdot \left[ k \cdot J_1\left(\frac{kr}{R}\right) - \frac{2R}{r} \cdot J_2\left(\frac{kr}{R}\right) + \frac{2R}{r} \cdot \xi \cdot J_2\left(\frac{hr}{R}\right) \right] \quad (3a)$$

$$V = \frac{A \cdot \sin(2\theta)}{R} \cdot \left[ -\frac{2R}{r} \cdot J_2\left(\frac{kr}{R}\right) - \xi \cdot \left( h \cdot J_1\left(\frac{hr}{R}\right) - \frac{2R}{r} \cdot J_2\left(\frac{hr}{R}\right) \right) \right] \quad (3b)$$

where  $k$  and  $h$  are the frequency parameters;  $\xi$  is the mode shape constant;  $J_1$  and  $J_2$  are the Bessel functions of the first kind; and  $A$  is the vibration amplitude, in the unit of squared meter.

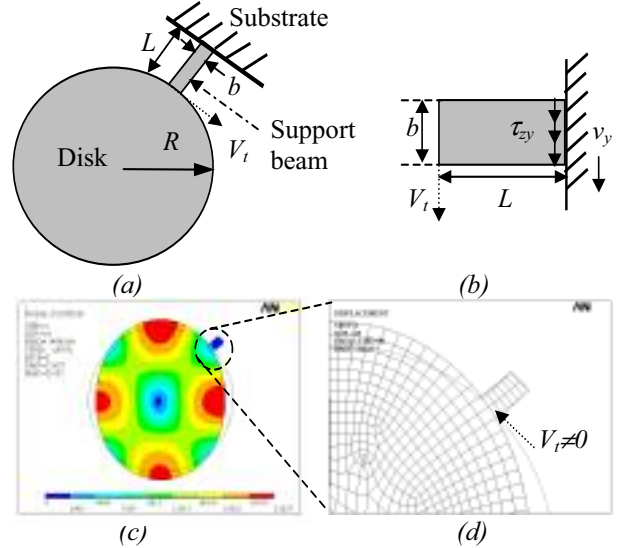


Figure 2. A side-supported disk resonator operating in its elliptic mode (a) top schematic view (b) support beam modeled as a cantilever (c) the elliptic mode (d) circumferential displacement

The angular resonant frequency and vibration energy of this mode are, respectively, expressed as:

$$\omega_{elliptic} = \frac{k}{R} \cdot \sqrt{\frac{E_d}{\rho_d \cdot (1 - \nu_d^2)}} \quad (4)$$

$$W_{elliptic} = \frac{\pi}{2} \cdot \rho_d \cdot t \cdot \omega^2 \cdot A^2 \cdot \Sigma \quad (5)$$

where  $\rho$ : density,  $E$ : Young's modulus,  $\nu$ : Poisson's ratio, and  $\Sigma$ : integral constant for the elliptic mode. Subscripts  $d$ ,  $s$ , and  $sub$  denote the materials used for the disk, support beam, and substrate, respectively.

As shown in Fig. 2(d), while the support beam is located at the resonant node with the radial displacement diminishing, the circumferential displacement at this node is non-zero, which can be calculated from Equation (3b) by substituting  $r$  with  $R$ :

$$V_t = \frac{A}{R} \cdot \left[ -2 \cdot J_2(k) - \xi \cdot (h \cdot J_1(h) - 2 \cdot J_2(h)) \right] \quad (6)$$

It is the non-zero circumferential displacement ( $V_t$ ) that introduces the bending motion at the disk end of the beam. Following this motion, the beam acts as a cantilever shown in Fig. 2(b) and results in the shear stress on the substrate [1]:

$$\tau_{zy} = \pi^4 \beta^4 \cdot \frac{E_s \cdot b^2 \cdot V_t \cdot A}{48 \cdot L^3 \cdot R} \quad (7)$$

where  $\beta$  is the mode constant related to a cantilever.

Based on the elastic wave theory and the Fourier transform [1], the mathematical expression for the displacement in the substrate due to the stress ( $\tau_{zy}$ ) is written as below:

$$v_y = \frac{4b}{\pi \cdot E_{sub}} \cdot \frac{1 + \nu_{sub}}{1 - \nu_{sub}} \cdot \Pi \cdot \tau_{zy} \quad (8)$$

where  $\Pi$  is an integral constant related to shear stress.

After the displacement incurred by the stress over the clamped region is determined, the amount of energy loss per cycle can be formulated as:

$$\Delta W_{side} = \pi \cdot \tau_{zy}^2 \cdot b \cdot t \cdot v_y \quad (9)$$

where the coefficient  $\pi$  is due to the time-harmonic nature of the stress and its corresponding displacement in the substrate.

By combining Equations (1) and (3) ~ (9), a closed-form expression for support quality factor ( $Q_{support}$ ) of a side-supported disk resonator can be written as (10) at the bottom of this page.

### Center-supported disk resonators

Fig. 3(a) shows a center-supported disk resonator of radius  $R$  and thickness  $t$ , suspended from the substrate through a beam of radius  $a$  and height  $h$ . With the support beam located at its center, which is coincident with the resonant node, the disk resonator operates in either its first or second radial mode, as shown in Figs. 3(c) and (d). Due to the lack of test data for the elliptic mode, only the radial modes are analyzed here.

Such radial mode shapes consist of solely the radial displacement ( $U$ ), expressed as below:

$$U_p = B \cdot J_1(\gamma_p \cdot r/R) \quad (11)$$

where  $\gamma_p$  is the frequency parameter;  $B$  is the vibration amplitude. Subscript  $p$  denotes the radial mode order.

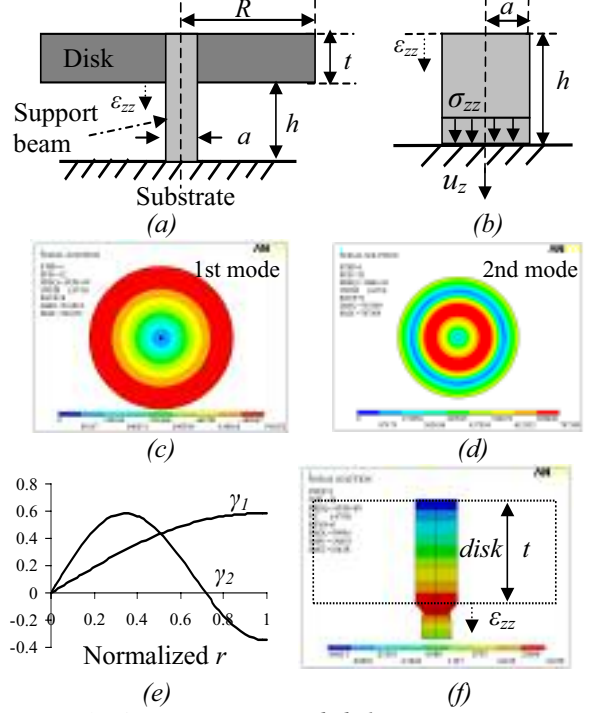


Figure 3. A center-supported disk resonator operating in its radial modes (a) side schematic view (b) support beam modeled as a longitudinal rod (c) the 1<sup>st</sup> radial mode (d) the 2<sup>nd</sup> radial mode (e) radial displacement along the radial direction (f) z-axis strain in the beam

The radial-mode angular resonant frequency and vibration energy are, respectively, expressed as:

$$\omega_{radial, p} = \frac{\gamma_p}{R} \cdot \sqrt{\frac{E_d}{\rho_d \cdot (1 - \nu_d^2)}} \quad (12)$$

$$W_{radial, p} = \frac{1}{2} \cdot E_d / (1 - \nu_d^2) \cdot \pi \cdot t \cdot \left[ \gamma_p \cdot B \cdot J_2(\gamma_p) \right]^2 \quad (13)$$

Although both the radial and circumferential displacements at the center of the disk are zero, the in-plane volume change in the disk causes the vertical strain perpendicular to the disk, as shown in Fig. 3(f). Following this strain, the center support beam acts as a longitudinal rod in Fig. 3(b), resulting in the normal stress on the substrate:

$$Q_{side-supported} = \frac{576 \cdot k^2 \cdot \Sigma}{\pi^6 \cdot \beta^8 \cdot V_t^2 \cdot \Pi} \cdot \left\{ \frac{E_d \cdot E_{sub} \cdot (1 - \nu_{sub})}{E_s^2 \cdot (1 - \nu_d^2) \cdot (1 + \nu_{sub})} \right\} \cdot \left( \frac{L}{b} \right)^6 \quad (10)$$

$$\sigma_{zz} = \frac{E_s \cdot v_s}{1 - v_s} \cdot \frac{2B}{a \cdot \cos(\frac{2\pi}{\lambda_s} \cdot h)} \cdot J_1(\gamma_p \cdot a/R) \quad (14)$$

where  $\lambda_s$  is the wavelength of the elastic wave in the beam, induced by the vibrations of the disk.

The displacement in the substrate due to the normal stress ( $\sigma_{zz}$ ) is calculated from the elastic wave theory:

$$u_z = \frac{8a}{E_{sub}} \cdot \frac{1 - v_{sub}^2}{1 - 2v_{sub}} \cdot \Psi \cdot \sigma_{zz} \quad (15)$$

where  $\Psi$  is an integral constant related to normal stress.

The amount of energy loss per cycle through the center support beam is further expressed as:

$$\Delta W_{center} = \pi \cdot \sigma_{zz}^2 \cdot \pi \cdot a^2 \cdot u_z \quad (16)$$

Thus, the combination of Equations (11) ~ (16) results in a closed-form expression for support quality factor of a center-supported disk resonator (17) shown at the bottom of this page.

### Design guidelines for high- $Q$

The analytical model derived here provides the design guidelines for achieving high- $Q$  in these resonators, which are summarized as below:

1) Choice of material: As illustrated in Equations (10) and (17), in order to increase  $Q_{support}$ , high-strength material is preferred for the disk and substrate (for higher vibration energy and lower support loss), while low-strength material for the support beam.

2) Geometrical dimensions

#### Side-supported disk resonators:

i)  $Q_{support}$  is independent of the disk dimensions ( $t$  and  $R$ ), indicating that the resonant frequency of a disk resonator can be decoupled from its  $Q_{support}$ .

ii) Thicker disk resonator will have reduced motional resistance, without changing  $Q_{support}$ .

iii) Although  $Q_{support}$  is highly sensitive to the beam dimensions  $(L/b)^6$  for the disks of same radius, the dependence of  $Q_{support}$  on the mode shape  $1/\beta^8$  of the support beam should be addressed here. Fig. 4 illustrates the flexural mode shapes of a support beam with varying lengths, showing that the support beam vibrates in its flexural mode shape, whose frequency approximates that of the disk. Since the mode constant

of the beam increases with its mode orders, large  $L/b$  may induce small  $1/\beta$ . The support beam dimensions should be chosen with care to avoid stiction and survive shock, while maximizing the  $Q_{support}$ .

#### Center-supported disk resonators:

i)  $Q_{support}$  decreases with the support beam radius ( $a$ ). This may be explained by the fact that smaller beams introduce less interference with vibrations in the disk.

ii) Thicker disks offer not only lower motional resistance but also higher  $Q_{support}$ . It needs to be noted that the ratio of  $t/a$  should ensure 2D plane stress for the validity of the above derivation.

iii)  $Q_{support}$  varies with the thickness ( $h$ ) of the beam periodically. The center support beam behaves as a transmission line due to its longitudinal motion. Hence, it is desirable to make the beam thickness equal to half of the elastic wavelength ( $h/\lambda_s=0.5$ ).

iv)  $Q_{support}$  decreases with the mode orders ( $p$ ), since the beam of the same radius has more interference with the higher-order modes, as shown in Fig. 3(e).

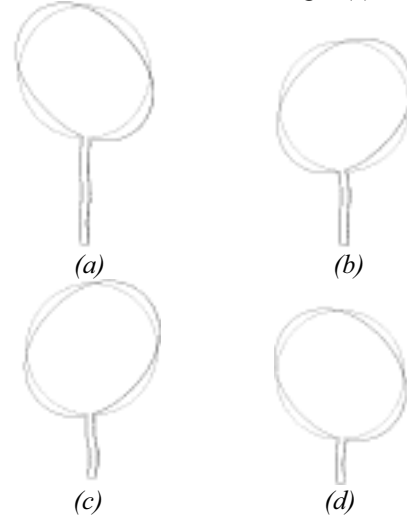


Figure 4. The resonant shapes of the support beam of a disk resonator of  $R=14.7\mu m$ . Beam width is fixed at  $b=1.7\mu m$ . (a)  $L=23.4\mu m$  (b)  $L=16.7\mu m$  (c)  $L=14\mu m$  (d)  $L=10\mu m$

### 3. EXPERIMENTAL VERIFICATION

In order to demonstrate its validity, this analytical model is compared with the experimental data. Fig. 5(a) shows a SEM picture of a side-supported SCS disk resonator, while Fig. 5(b) illustrates its exact beam dimensions to characterize support loss. The measured

$$Q_{center - supported} = \left\{ \frac{E_d \cdot E_{sub} \cdot (1 - 2v_{sub}) \cdot (1 - v_s)^2}{32 \cdot E_s^2 \cdot v_s^2 \cdot (1 - v_d^2) \cdot (1 - v_{sub}^2)} \right\} \cdot \frac{t \cdot \cos^2(2\pi \cdot h / \lambda_s)}{a \cdot \Psi} \cdot \left( \frac{\gamma_p \cdot J_2(\gamma_p)}{J_1(\gamma_p \cdot a/R)} \right)^2 \quad (17)$$

resonant frequency and the quality factor of this disk resonator are illustrated in Fig. 5(d). A  $10\mu\text{m}$ -thick disk resonator shown in Fig. 5(c) offers a lower motional resistance but same  $Q_{\text{support}}$  [2].

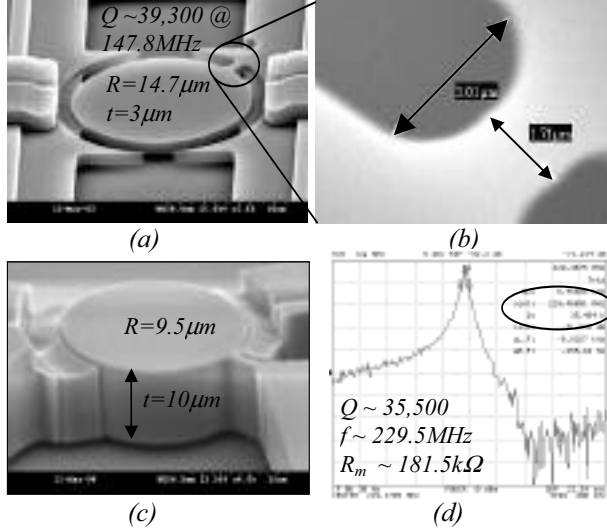


Figure 5. Side-supported disk resonators (a)  $3\mu\text{m}$ -thick disk resonator (data used in row 3 of Table 1) (b) beam dimensions (c)  $10\mu\text{m}$ -thick disk resonator (d) frequency response of the disk resonator in (c) (data used in row 1 of Table 1,  $R_m$ : motional resistance)

Table 1 lists the measured quality factors ( $Q_{\text{measured}}$ ) and calculated  $Q_{\text{support}}$  of the elliptic mode of different sizes of side-supported SCS disk resonators operating in vacuum, showing that  $Q_{\text{support}}$  is independent of the disk thickness (highlighted rows). Table 2 compares the  $Q_{\text{measured}}$  with calculated  $Q_{\text{support}}$  of the radial modes of different center-supported poly-diamond disk resonators with their support beams made from polysilicon (data taken from [3]), indicating that  $Q_{\text{support}}$  decreases with the mode orders. Taking experimental and fabrication tolerance into account, the analytical model demonstrates good agreement with the measured data.

Table 1. Comparison between the measured quality factor ( $Q_{\text{measured}}$ ) [2] and the calculated  $Q_{\text{support}}$  for side-supported disk resonators operating in vacuum

R ( $\mu\text{m}$ )	L ( $\mu\text{m}$ )	b ( $\mu\text{m}$ )	t ( $\mu\text{m}$ )	f (MHz)	$Q_{\text{measured}}$	$Q_{\text{support}}$
9.5	3.4	2	10	229.5	35,500	33,848
14.5	3.85	2.1	10	150	48,800	53,247
14.7	3	1.7	3	147.8	39,300	41,712
15	3.5	1.9	18	149.3	45,700	54,794
15	8	5.8	4.5	149.3	7,907	9,656
25	5.5	3	4.5	75.57	42,000	53,247

#### 4. CONCLUSION

An analytical model has been developed for support loss in micromechanical disk resonators, providing

closed-form expressions for  $Q_{\text{support}}$  and design guidelines for achieving high- $Q$  in such resonators. The validity of this model has been verified with the experimental data. Strong dependence of  $Q_{\text{support}}$  on the material properties suggests high-strength material for the disk and substrate while soft material for the beam. While  $Q_{\text{support}}$  in side-supported disks is associated with the beam size and independent of the disk dimensions,  $Q_{\text{support}}$  in center-supported disks depends on both the disk and beam dimensions.

Table 2. Comparison between the  $Q_{\text{measured}}$  [3] and the calculated  $Q_{\text{support}}$  for center-supported disk resonators ( $h=0.8\mu\text{m}$ ,  $t=3\mu\text{m}$ ) (a) the 1<sup>st</sup> (b) the 2<sup>nd</sup> radial modes

R ( $\mu\text{m}$ )	a ( $\mu\text{m}$ )	f (MHz)	$Q_{\text{measured}}$	$Q_{\text{support}}$
12	0.8	455.8	24,117	28,161
10	1	547.2	11,448	9,717
10	0.8	545.9	17,458	18,913
8.5	0.85	639.2	10,531	10,929

R ( $\mu\text{m}$ )	a ( $\mu\text{m}$ )	f (MHz)	$Q_{\text{measured}}$	$Q_{\text{support}}$
12	0.8	1272.2	12,050	15,601
11	0.8	1388.1	10,680	11,321
11	1	1386.9	8,760	5,813
10	1	1519.7	4,648	3,913

#### ACKNOWLEDGMENT

The authors wish to thank Siavash Pourkamali for providing the experimental data. This work is supported by DARPA NMAPS program.

#### REFERENCES

- [1] Z. Hao, A. Erbil, and F. Ayazi, "An Analytical Model for Support Loss in Micromachined Beam Resonators with In-plane Flexural Vibrations", *Sensors and Actuators A*, Vol. 109, 2003, pp. 156-164.
- [2] S. Pourkamali, and F. Ayazi, "High Frequency Capacitive Micromechanical Resonators with Reduced Motional Resistance Using the HARPSS Technology", *the 5<sup>th</sup> Silicon RF Topical Meeting 2004*, pp. 147-150.
- [3] J. Wang, J. E. Butler, Tatyana, and C. T. Nguyen, "1.51-GHz nanocrystalline diamond micromechanical disk resonator with material-mismatched isolating support", *Proc. MEMS 2004*, pp. 641-644.
- [4] Z. Hao, A. Erbil, and F. Ayazi, "Thermoelastic Damping in Micro- and Nanomechanical Circular Thin-plate Resonators", to be published.
- [5] Z. Hao, S. Pourkamali, and F. Ayazi, "VHF Single Crystal Silicon Elliptic Bulk-mode Capacitive Disk Resonators Part I: Design and Modeling", *JMEMS*, Dec. 2004.
- [6] S. Pourkamali, Z. Hao, and F. Ayazi, "VHF Single Crystal Silicon Elliptic Bulk-mode Capacitive Disk Resonators Part II: Implementation and Characterization", *JMEMS*, Dec. 2004.